

Late Quaternary terrigenous sedimentation in the Western Arctic Ocean as exemplified by a sedimentary record from the Alpha Ridge

LIU Weinan¹, WANG Rujian^{1*}, CHEN Jianfang², CHENG Zhenbo³, CHEN Zhihua³
& SUN Ye Chen¹

¹State Key Laboratory of Marine Geology, Tongji University, Shanghai 200092, China;

²The Second Institute of Oceanography, SOA, Hangzhou 310012, China;

³The First Institute of Oceanography, SOA, Qingdao 266062, China

Received August 5, 2011; accepted November 1, 2011

Abstract Terrigenous components in sediment core B84A from the Alpha Ridge, Western Arctic Ocean, have been investigated to reconstruct Mid to Late Quaternary variations in sedimentation, provenance, and related climate changes. The core stratigraphy, evaluated by a combination of variations in Mn content, color cycles, foraminiferal abundance, and lithological correlation, extends back to estimated Marine Isotope Stage 12. Twelve Ice Rafted Detritus (IRD, >250 μm) events were identified and interpreted to mostly occur during deglaciation. The Canadian Arctic, which was covered by ice sheets during glacial periods, is suggested to be the major source region. The IRD events likely indicate the collapses of ice sheets, possibly in response to abrupt climate changes. Grain size analysis of B84A indicates sedimentologically sensitive components in core B84A in the 4–9 μm and 19–53 μm silt subfractions, which are inferred to be mainly transported by currents and sea ice, respectively. Down core variability of these two fractions may indicate changes in ice drift and current strength. In accordance with previous studies in the central Arctic Ocean, the average sedimentation rate in core B84A is about 0.4 $\text{cm}\cdot\text{ka}^{-1}$. Compared with the relatively high sedimentation rates on the margins, sedimentation in the central Arctic Ocean is limited by sea ice cover and the correspondingly low bioproductivity, as well as the long distance from source regions of terrigenous sediment.

Keywords IRD event, terrigenous component, sedimentation rate, Arctic Ocean, Alpha Ridge, Quaternary

Citation: Liu W N, Wang R J, Chen J F, et al. Late Quaternary terrigenous sedimentation in the Western Arctic Ocean as exemplified by a sedimentary record from the Alpha Ridge. *Adv Polar Sci*, 2011, 22: 215–222, doi: 10.3724/SP.J.1085.2011.00215

0 Introduction

The Arctic Ocean, the smallest ocean on the Earth, is bounded by the Eurasian and North American continents. The Arctic Ocean is characterized by large shelf areas and the deep Eurasian (east) and Canadian (west) basins. The Transpolar Current in the Eurasian Basin

and the clockwise circulating Beaufort Gyre in the Canadian Basin constitute the two major surface ocean circulations in the Arctic Ocean. The currents can control the distribution of sediments in the Arctic Ocean directly or through drifting sea ice and icebergs, which transport terrigenous material known as Ice Rafted Detritus (IRD).

Liu Weinan (born in 1987, male, PhD student, marine geology, email: liuweinan.lwn@gmail.com)

*Corresponding author (email: rjwang@tongji.edu.cn)

Deposition of IRD is also related to the stability of ice sheets surrounding the Arctic Ocean during glacial periods. Ice-sheet collapse events are documented by IRD peaks in the sedimentary record. When tracked across the basin, these events provide valuable information on the condition of ice sheets and the concomitant Arctic circulation^[1]. IRD provenance studies indicate that icebergs in the Eastern Arctic originate mostly from the Eurasian ice sheets^[2]. Ice-rafted deposits in the Western Arctic show prevailing contributions from Canadian Arctic sources including several iceberg events during the last deglaciation^[3–4]. This study aims to reconstruct the Quaternary history of IRD events, variations in sedimentation, source regions, and related climate changes by focusing on the coarse IRD and finer sediment grain size in core B84A recovered from the Alpha Ridge, Western Arctic Ocean, during the third Chinese National Arctic Expedition in 2008.

1 Material and methods

Gravity core B84A (143°34.83'W, 84°26.54'N, 2 280 m water depth) was recovered from the Alpha Ridge (Figure 1). A total of 94 samples were taken from the 186 cm core at 2 cm intervals. The sediments show clear changes in color (Figure 2) and lithological features.

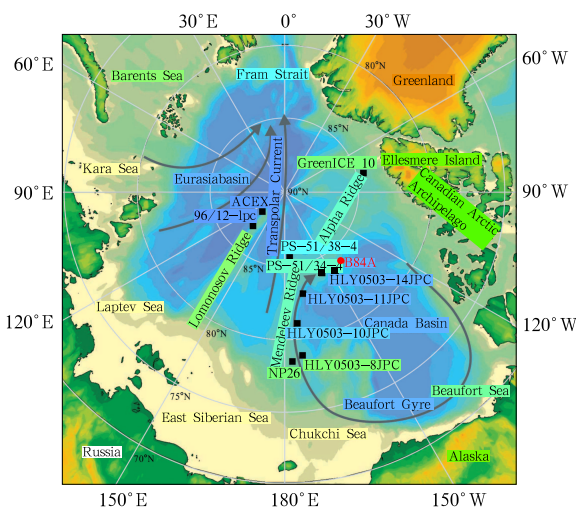


Figure 1 Arctic Ocean map with location of core B84A and cores from earlier studies cited^[2,5–6]. Arrows show major surface currents in the Arctic Ocean.

Several parameters were measured on core B84A including color reflectance, XRF element counts, coarse IRD (>250 μm) content, foraminifera abundance,

AMS ^{14}C dating and sediment grain size. All analyses, except for the AMS ^{14}C dating, were carried out at the State Key Laboratory of Marine Geology, Tongji University, China, and the AMS ^{14}C dating was carried out in University of California, USA.

Sediment color reflectance was measured using the Minolta CM2002 reflectance meter. The results were expressed in three parameters (L^* , a^* and b^*). Elemental composition was measured using the AVAATECH® non-destructive X-ray Fluorescence (XRF) core scanner on the split half core at 1 cm resolution. Measurements were carried out at 10 kV, 30 kV and 50 kV, with a measurement time of 30 s for each energy level, to register a wide range of elements (Al to U). The data are represented as counts/30 s.

For foraminiferal abundance and IRD content, 10–15 g of dry sediment was wet rinsed through a $\Phi 63\text{-}\mu\text{m}$ mesh. Then the dried and weighed >63 μm fraction was dry sieved through meshes of $\Phi 154$ and $\Phi 250 \mu\text{m}$, successively, and each fraction was weighed. Foraminifera in the >154 μm fraction were separated and counted under the microscope. IRD (>154 and 250 μm) contents were calculated by removing the weights of foraminifera.

For grain size measurement, organic material, CaCO_3 and biogenic silica were removed from 0.15 g of dry sediment by using H_2O_2 , HCl and NaOH, respectively. Grain size was measured on the processed sediment with the Coulter Automatic Laser Analyzer.

2 Core stratigraphy

The discontinuous record of foraminifera in the central Arctic Ocean due to low biological productivity and poor preservation, as well as a strong local freshwater signal prevents the application of conventional oxygen isotope stratigraphy^[7]. Alternative proxies have been evaluated in several studies such as variations in manganese (Mn) content and color reflectance of deep sea sediments in the central Arctic Ocean^[7,10]. Together with several biostratigraphic events^[8], the developed chronology suggests that gray units generally represent glacial periods and brown units represent warm stages^[6,9–12].

Precipitation of manganese in Arctic sediments is mainly controlled by terrigenous inputs (mostly riverine)^[13] and, possibly, the relative degree of ventilation of Arctic Ocean waters^[10–11] related to glacial-interglacial cycles. Mn-rich intervals have been associ-

ated with warm stages with reduced sea ice cover and increased riverine inputs^[9]. Color reflectance can be expressed by three parameters: luminance or relative brightness (L^*), the green-to-red color range (a^*), and the blue-to-yellow color range (b^*). The a^*/b^* ratio can be used as a proxy for sediment color changes, which may reflect changes in sediment composition^[11]. Brownish-yellowish to grayish color cycles in Arctic Ocean sediments are considered to represent interglacial/glacial cyclicity^[9–10,13]. In this model, brownish-yellowish sediments indicate interglacial or interstadial environments with relatively high productivity and open water conditions, and possibly enhanced Atlantic water inflow and bottom water ventilation. Grayish sediments indicate extended ice cover and reduced bioproductivity in glacial environments, possibly combined with a weakened Atlantic water inflow and bottom water ventilation^[5–6,11–12]. Thus, glacial and warm stages can be approximated by the results of L^* and a^*/b^* measurements. Sediment color in core B84A clearly varies with core depth (Figure 2). Brownish-yellowish intervals correspond to high values of a^*/b^* and Mn content, and to low values of L^* , indicating warm stages. Grayish intervals correspond to low values of a^*/b^* and Mn content and high values of L^* , indicating glacial deposition. In addition, high foraminiferal abundance intervals

in the upper part of the Quaternary record correspond to warm, high productivity periods^[6]; however, further down core, calcareous foraminifera are usually not preserved.

To better constrain the stratigraphy based on lithological features, core B84A was correlated to core PS51/38–4 from the Alpha Ridge^[10]. The Ca content (XRF counts) of core B84A was also correlated to the Ca content of adjacent core HLY0503–14JPC (hereafter 14JPC) dated with amino-acid racemization (AAR)^[6] (Figure 2).

The lithological features and color changes of core B84A were correlated to those of core PS51/38–4 (Figure 2). The basal brown layers B1 and B2 were dated at ca.11 and 45 ka, respectively^[6,12,15]. The base age of B1 is reasonably in agreement with the AMS ^{14}C age dating on *Neogloboquadrina pachyderma* (Nps) in core B84A (15 ka, Wang et al., unpubl. data). However, the white layer W3 above B2 was not recognized in core B84A.

The Ca content of core B84A can be correlated well to that of core 14JPC^[6] (Figure 2). The Ca content usually does not covary with the planktic foraminiferal abundance in the Arctic Ocean. This is because the Ca content primarily represents detrital carbonates, whereas the foraminiferal contribution is negligible^[6]. The second Ca spike yields an AAR age of 47 ka in core 14JPC^[6],

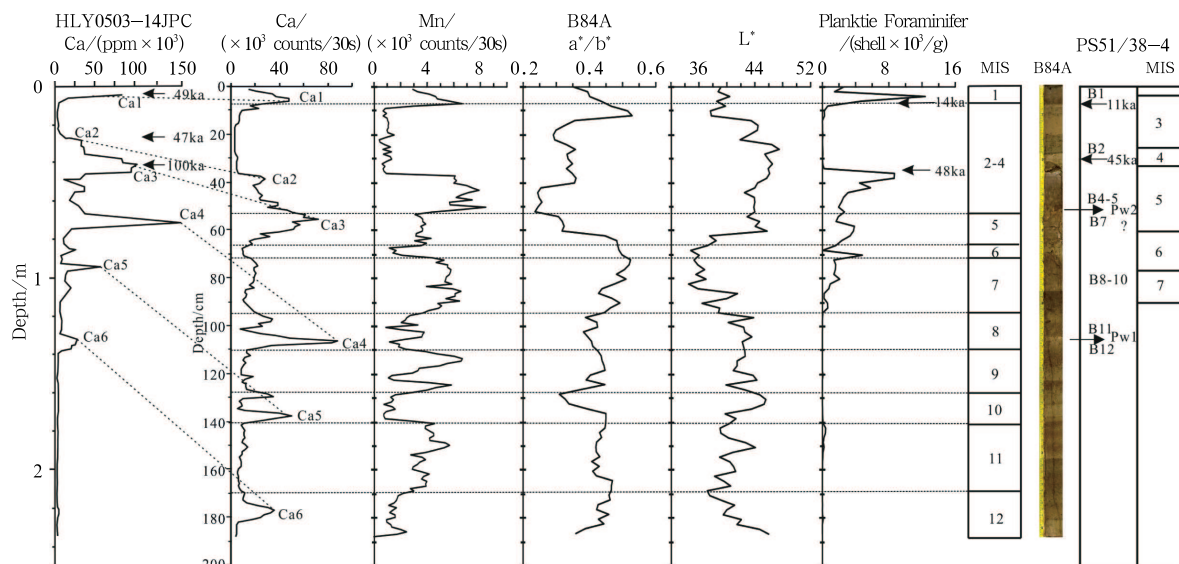


Figure 2 Ca content, Mn content, color reflectance, and foraminiferal abundance of core B84A, correlated to Ca content of core HLY0503–14JPC^[6]. The Ca spikes for correlation are marked. The lithological features (and color units) of core B84A were correlated to those of core PS51/38–4^[11]. The AAR ages for core 14JPC^[6], estimated ages for lithological intervals^[10] and AMS ^{14}C ages for B84A are marked. MIS: Marine Isotope Stage.

agreeing well with the AMS ^{14}C age (Nps) in core B84A (48 ka, Wang et al., unpubl. data). The interval of Ca spike 3 was dated at ca. 100 ka by AAR ages in different cores^[6], constraining the lower part of Marine Isotope Stage (MIS) 5. An expected pink-white layer (PW2) at this interval is not observed^[10]. However, the Ca spike and relatively low planktonic foraminifera abundance indicate that a similar lithological feature proposed for PW2, dated at MIS 5 d^[10], also is in agreement with the AAR age in core 14JPC. A pink-white layer was found at a core depth of 105–107 cm (Figure 2), corresponding to Ca6, which we assumed to be the PW1 layer in other central Arctic cores^[6,10], with a proposed age of MIS8^[11].

In summary, the stratigraphy of core B84A is developed based on the combination of lithological feature correlations, Ca content, Mn content, color cycles and

foraminiferal abundance. Marine isotope stages (MIS) are tentatively assigned to the core by correlation of the above proxies to the Ca content of core HLY0503–14JPC^[6] (Figure 2).

3 Results

3.1 Sedimentation rates

According to the proposed age model, sedimentation rates in core B84A are estimated for different MIS (Table 1). The average sedimentation rate in the core is approximately $0.4 \text{ cm}\cdot\text{ka}^{-1}$. In general, sedimentation rates during interglacial periods appear to be greater than during glacial periods, which may be related to very low deposition under expanded ice during glaciations. The low sedimentation rate in MIS 6 may result from the sedimentary hiatus and still needs further study.

Table 1 Estimated sedimentation rates in core B84A during the identified glacial and interglacial periods

Glacial MIS	2–4	6	8	10	12	average
Sedimentation rate/($\text{cm}\cdot\text{ka}^{-1}$)	0.7	0.1	0.3	0.3	0.3	0.41
Interglacial MIS	1	5	7	9	11	average
Sedimentation rate/($\text{cm}\cdot\text{ka}^{-1}$)	0.6	0.3	0.4	0.4	0.6	0.37

3.2 IRD content and grain size

The IRD ($>250 \mu\text{m}$) content in core B84A varies between 0.3% and 18% of sediment weight, with an average of 3.4%. Twelve IRD events, defined by values $>5\%$, can be recognized in this core including four major events with an IRD content of $\sim 10\%$ or higher (Table 2). The average IRD content during the identified glacial periods (MIS 2–4, 6, 8, 10, 12) is higher than during interglacials (MIS 1, 5, 7, 9, 11) (Figure 3).

The distribution of the standard deviation of grain size^[16] has been analyzed in core B84A to identify sedimentologically sensitive grain components. The distribution shows a bimodal pattern (Figure 4a). Sensitive grain size components are identified in a fine silt range of

$4\text{--}9 \mu\text{m}$ and a coarse silt range of $19\text{--}53 \mu\text{m}$, peaking at $6 \mu\text{m}$ and $27 \mu\text{m}$, respectively. The insensitive grain size component is in the range of $10\text{--}13 \mu\text{m}$. The two sensitive fractions vary differently down core (Figure 4b). The peaks of IRD content and median grain size correspond to the increase in the coarse sensitive component.

Based on a statistical analysis of grain size in the glacial and interglacial intervals, mean and median grain sizes and average content of sand fraction ($>63 \mu\text{m}$) are observed to be higher during glacial periods (MIS 2–4, 6, 8, 10, 12). In contrast, the average silt ($2\text{--}63 \mu\text{m}$) and clay ($<2 \mu\text{m}$) fractions are greater during interglacials (MIS 1, 5, 7, 9, 11). Because a collapsing ice sheets may input most of its terrigenous sediment during deglaciations, we assume that deposition of coarser fractions is

Table 2 IRD events ($>5\%$) in core B84A

depth/cm	0–2	12–16	26	34	68	80
IRD event	1	2	3	4	5	6
IRD content/%	9.9	6.5–7.5	7.1	12.3	6.4	18.2
Depth /cm	94–98	104	120	126	134–136	174–176
IRD event	7	8	9	10	11	12
IRD content /%	6.9–7.9	7.6	5.3	5.3	5.6–7.1	10.6

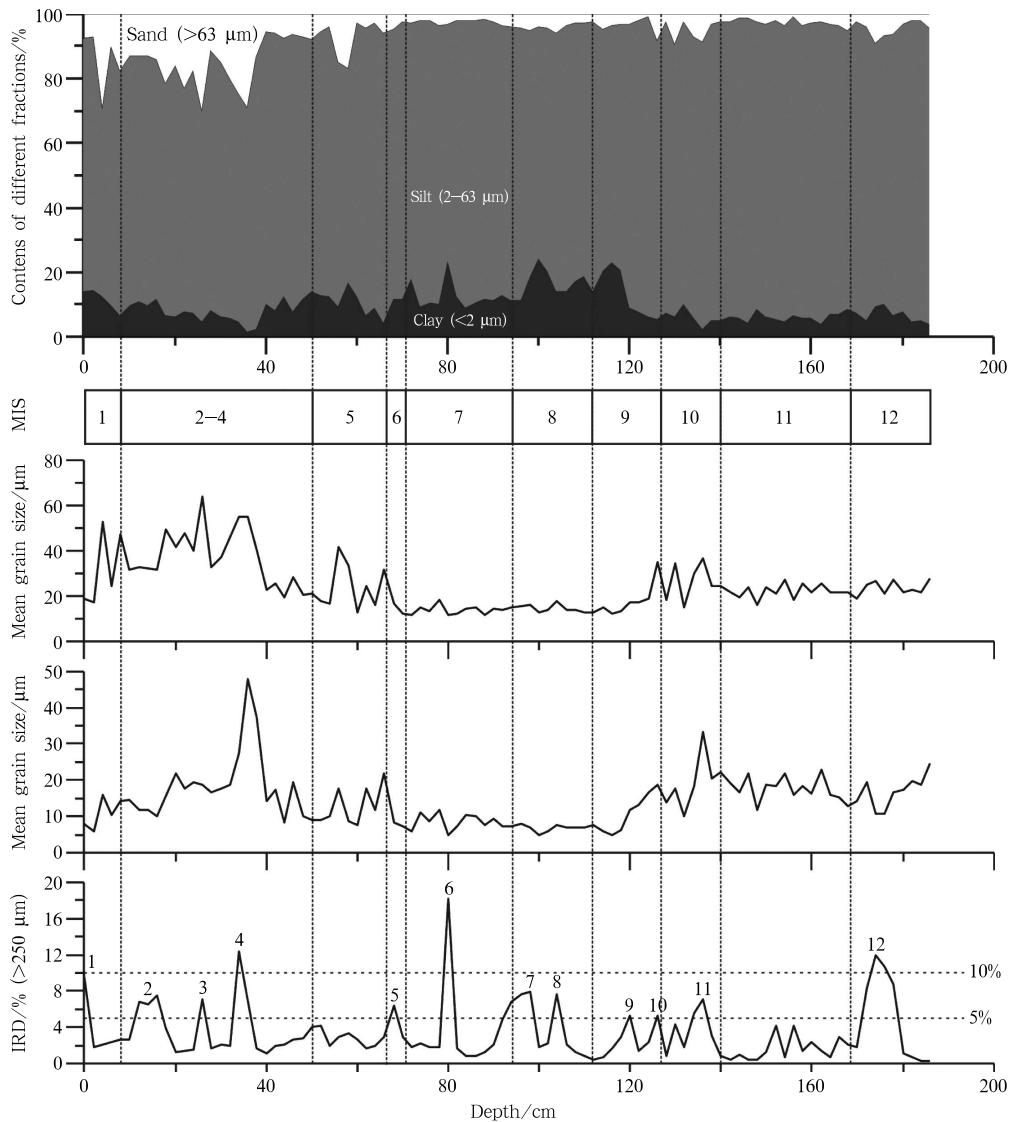


Figure 3 Down core distribution of major grain size fractions, mean and median grain sizes, and the IRD content in core B84A.

higher during periods of deglaciation rather than full-glacial intervals.

4 Discussion

4.1 IRD events and provenance

Previous studies show that coarse fractions (sand or coarser IRD) are mostly carried by icebergs^[17–18]. Investigations of late Quaternary IRD occurrences in the Western Arctic Ocean indicate that the content of coarse fractions is relatively low in interglacial sediments and high in the glacial and deglacial sediments^[19–20]. Other than near the continental margins, deposition of IRD in

the Arctic Ocean mainly has occurred during deglacial periods, when ice sheets disintegrated and icebergs could circulate more freely across the central Arctic Ocean^[21]. This is generally in agreement with the B84A record that appears to indicate more IRD during deglacial rather than full glacial intervals. The relatively high IRD content in the uppermost sediment in the core may have resulted from iceberg discharge during the last deglaciation.

The distribution pattern of IRD in the surface sediments of the Western Arctic Ocean indicates Northwestern Canada (coastal Beaufort Sea) as the main source region, from which ice is transported by the Beaufort

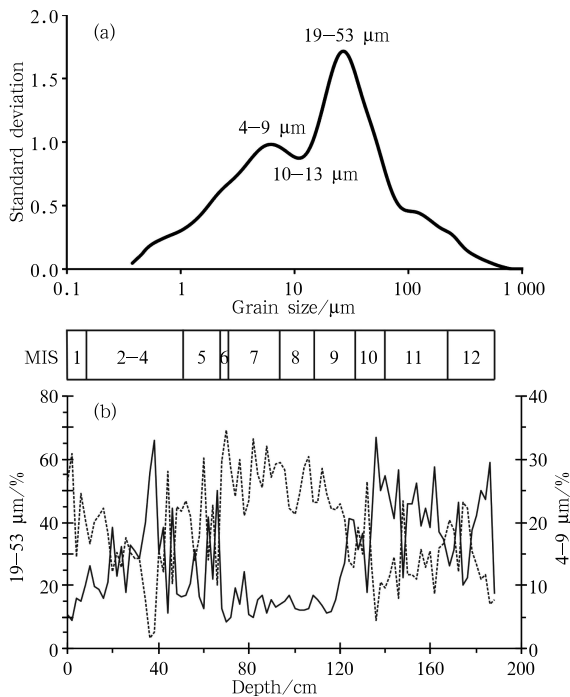


Figure 4 Standard deviation of grain size (a) and down core distribution of sensitive grain size components (19–53 μm , solid line, and 4–9 μm , dotted line) (b) in core B84A.

Gyre^[21]. However, during glacial times, when icesheets expanded on the Eurasian and North American continents^[22–23], a major source region for the Alpha Ridge could be the Canadian Arctic Archipelago and more distant areas of the Canadian shield impacted by the Laurentide ice sheet^[10,19,24]. Ice drift from the Arctic Russian shelves also may have contributed, because the position of the Transpolar Current was shifted relative to its present position such that it extended into the Western Arctic Ocean^[11,19]. These patterns are supported by the IRD distribution and related sedimentary features in multiple cores from the Western Arctic Ocean. For example, six IRD events in core GreenICE 10 from the Lomonosov Ridge during MIS 1–7^[20] can be correlated readily to IRD events in core B84A. Lithologic features of cores HLY0503–14JPC and PS51/38–4 (Figure 2)^[6,11] are also similar to core B84A in the latest two glacial/interglacial cycles. In summary, during interglacial periods, under a circulation pattern similar to today, IRD volume was low and likely transported to the Alpha Ridge by the Beaufort Gyre from the coastal Beaufort Sea, possibly with a contribution from Siberian shelves. During glacial/deglacial periods, higher amounts of IRD were deposited and the Canadian

Arctic Archipelago covered by the Laurentide ice sheet became the main source region. Further identification of the IRD source areas will be performed in a future study of the geochemical composition of the sediments.

The IRD content does not always covary with the grain size of finer sediment (Figure 3), which may be due to different sample sizes. The IRD was separated from only 10–15 g of sediment, so the small sample size for the grain size analysis (0.15 g) might not be sufficiently representative of large IRD content.

The coarse IRD ($>250 \mu\text{m}$) often appears in spikes, which are probably related to iceberg discharge events during glacial/deglacial periods^[2–3,25]. Previous studies show that the sediment texture of the fine fraction ($<45 \mu\text{m}$) in the central Arctic basins is similar to that in the shelf areas, indicating sea ice transport of these fine materials to the central Arctic^[26]. The frequent IRD events and increased coarse fraction also are indicated by mean and median grain size values (Figure 3) during glacial periods/cold stadials, especially MIS 2–4, and they may result from the instability of the surrounding ice sheets. The two sensitive subfractions (4–9 μm and 19–53 μm) vary asymmetrically. The down core variation of these subfractions may indicate changes in sediment sorting and the strength of related transportation pathways (current and sea ice drifting). The interpretation of the variability in this system needs further study.

4.2 Sedimentation rate comparison

The late Quaternary sedimentation rate in the Arctic Ocean varies from $>30 \text{ cm}\cdot\text{ka}^{-1}$ on the Alaskan margin to less than $1 \text{ cm}\cdot\text{ka}^{-1}$ in the Western Arctic basin^[6,24–25,27]. The average sedimentation rate of approximately $0.4 \text{ cm}\cdot\text{ka}^{-1}$ for core B84A is in the range of the previous estimations for the Alpha Ridge and adjacent areas^[2,5–6,27] (Table 3). An average sedimentation rate of $\sim 0.41 \text{ cm}\cdot\text{ka}^{-1}$ for the glacial periods in B84A is slightly lower than that of $\sim 0.37 \text{ cm}\cdot\text{ka}^{-1}$ for interglacial periods. This may result from the relatively high sedimentation rate for the warm periods of MIS 3, which was not separated from the cold MIS 2–4. Moreover, MIS 4 (and probably part of upper MIS 5) may be strongly condensed or even missing, due to the occurrence of planktic foraminifera and relatively good ventilation (as indicated by Mn) (Figure 2). The comparison of individual interglacial and glacial periods indicates a general pattern of

Table 3 Comparison of sedimentation rates of core B84A with other cores in the adjacent area^[6]

Cores	GreenICE	NP26	ACEX	HLY0503-8JPC	PS-51/38-4
Sedimentation rate/(cm·ka ⁻¹)	0.7	1	1.45	2	0.7
Cores	HLY0503-10JPC	HLY0503-11JPC	PS51/34-4	B84A	HLY0503-14JPC
Sedimentation rate/(cm·ka ⁻¹)	0.3	0.3	0.17	0.4	0.3

higher interglacial sedimentation rate than glacial sedimentation rate.

Sedimentation rates in the Western Arctic Ocean during the Holocene show 0.3–2 cm·ka⁻¹ and 0.2–5 cm·ka⁻¹ on the Mendeleev Ridge and the Northwind Ridge, respectively, but can be over 30 cm·ka⁻¹ near the Alaskan margin^[6]. Differences in sedimentation rates between the central Arctic Ocean and marginal areas are controlled by ocean circulation, ice cover and related bioproductivity, and terrigenous inputs. Sedimentation rates generally decrease under permanent sea ice and increase towards the ice margin^[6] because of higher release of sediment from melting ice and enhanced bioproductivity, together with higher terrigenous inputs from more closely located source regions. The sedimentation rate distribution pattern in the Western Arctic Ocean also indicates the major control that the Beaufort Gyre holds over sediment deposition.

5 Conclusion

Several proxies have been investigated in core B84A from the Alpha Ridge, Western Arctic Ocean, including Ca and Mn content, color reflectance, foraminiferal abundance, coarse IRD content, and detailed grain size.

A stratigraphic framework for core B84A has been developed based on the Mn content, Ca content, color reflectance, and foraminiferal abundance cyclicity compared with earlier established Arctic Ocean stratigraphies. The new stratigraphic framework suggests that core B84A covers the depositional interval from MIS 12 to MIS 1.

Twelve IRD events are recognized in core B84A for all stratigraphic units since MIS 12, except for the warm intervals estimated as MIS 5 and 11. These IRD events appear to have occurred mostly in deglacial periods. The coarse IRD may have mainly come from icebergs discharged from ice sheets covering the Canadian Arctic. The smaller size fractions that prevail in interglacial periods may have been mostly transported to the Alpha Ridge by sea ice in the Beaufort Gyre circulation system.

The grain size analysis performed as part of this work primarily highlights changes in the fine fractions. The most sensitive components are two silt subfractions, 19–53 μm and 4–9 μm . We infer that these subfractions are mainly transported by sea ice rafting and currents. The down core variability in these components may indicate changes in the patterns of sea-ice drift and/or current strength.

The average sedimentation rate in core B84A is approximately 0.4 cm·ka⁻¹, in agreement with previous studies in the central Arctic Ocean. Compared with relatively high sedimentation rates near the continental margins, sedimentation rates in the central Arctic Ocean are limited by sea ice cover and related low bioproductivity, as well as lower terrigenous input from distant source regions.

Acknowledgments This work is funded by the National Basic Research Program of China (Grant no. G2007CB815903), the National Natural Science Foundation of China (Grant nos. 41030859, 40321603), the China Program for International Polar Year 2007–2008, and the China Geological Survey project (Grant no. H[2011]01-14-04). We thank three anonymous referees for reviewing the manuscript, and providing helpful comments and suggestions. This work is part of the project “Third Chinese National Arctic Research Expedition” (the 3rd CHINARE-Arctic in 2008) supported by the Ministry of Finance of China and organized by the Chinese Arctic and Antarctic Administration (CAA), SOA, with participants from various Chinese institutions. The participants in the joint work are from several institutions (e.g., PRIC, FIO, SIO, Tongji University, etc.). Xue Bing, Lei Jijiang, Zhang Tao and Chen Jigan are appreciated for their work on core recovery. Also acknowledged are Wang Kunshan and Huang Yuanhui, and the polar sample repository of the Polar Research Institute of China (PRIC), for providing the core color reflectance and lithological descriptions. Samples information and data issued by the Resource-sharing Platform of Polar Samples (<http://birds.chinare.org.cn>) maintained by PRIC and Chinese National Arctic & Antarctic Data Center (CN-NADC). Samples provided by the Polar Sediment Repository of PRIC. Data issued by the Data-sharing Platform of Polar Science (<http://www.chinare.org.cn>) maintained by PRIC and CN-NADC.

References

- 1 Darby D A, Polyak L, Bauch H A. Past glacial and inter-

- glacial conditions in the Arctic Ocean and marginal seas—a review. *Progress in Oceanography*, 2006, 71: 129-144
- 2 Spielhagen R, Baumann K, Erlenkeuser H, et al. Arctic Ocean deep-sea record of northern Eurasian ice sheet history. *Quat Sci Rev*, 2004, 23: 1455-1483
 - 3 Darby D A, Bischof J F, Spielhagen R F, et al. Arctic ice export events and their potential impact on global climate during the late Pleistocene. *Paleoceanography*, 2002, 17: 2, doi: 10.1029/2001PA000639
 - 4 Darby D A, Zimmerman P. Ice-rafted detritus events in the Arctic during the last glacial interval and the timing of the Innuitian and Laurentide ice sheet calving events. *Polar Res*, 2008, 27: 114-127
 - 5 Backman J, Jakobsson M, Løvlie R, et al. Is the central Arctic Ocean a sediment starved basin? *Quat Sci Rev*, 2004, 23: 1435-1454
 - 6 Polyak L, Bischof J, Ortiz J D, et al. Late Quaternary stratigraphy and sedimentation patterns in the Western Arctic Ocean. *Global and Planetary Change*, 2009, 68: 5-17
 - 7 Darby D A, Bischof J F, Spielhagen R F, et al. Arctic ice export events and their potential impact on global climate during the late Pleistocene. *Paleoceanography*, 2002, 17: 2, doi: 10.1029/2001PA000639
 - 8 Backman J, Fornaciari E, Rio D. Biochronology and paleoceanography of late Pleistocene and Holocene calcareous nannofossil abundances across the Arctic Basin. *Mar Micropal*, 2009, 72: 86-98
 - 9 Jakobsson M, Løvlie R, Al-Hanbali H, et al. Manganese and color cycle in Arctic Ocean sediments constrain Pleistocene chronology. *Geology*, 2000, 28: 23-26
 - 10 Stein R, Matthiessen J, Niessen F. Re-Coring at ice island T3 site of key Core FL-224 (Nautilus Basin, Amerasian Arctic): sediment characteristics and stratigraphic framework. *Polarforschung*, 2010, 79 (2): 81-96
 - 11 Stein R, Matthiessen J, Niessen F, et al. Towards a better (litho-) stratigraphy and reconstruction of Quaternary paleoenvironment in the Amerasian Basin (Arctic Ocean). *Polarforschung*, 2010, 79 (2): 97-121
 - 12 Polyak L, Curry W B, Darby D A, et al. Contrasting glacial/interglacial regimes in the Western Arctic Ocean as exemplified by a sedimentary record from the Mendeleev Ridge. *Palaeogeogr Palaeoclimatol Palaeoecol*, 2004, 203: 73-93
 - 13 Löwemark L, Jakobsson M, Mörth M, et al. Arctic Ocean manganese contents and sediment color cycles. *Polar Res*, 2008, 27: 105-113
 - 14 Phillips R L, Grantz A. Quaternary history of sea ice and paleoclimate in the Amerasia basin, Arctic Ocean, as recorded in cyclical strata of Northwind Ridge. *Geological Society of America Bulletin*, 1997, 109: 1101-1115
 - 15 Adler R E, Polyak L, Ortiz J D, et al. Sediment record from the Western Arctic Ocean with an improved Late Quaternary age resolution: HOTRAX core HLY0503-8JPC, Mendeleev Ridge. *Global and Planetary Change*, 2009, 68: 18-29
 - 16 Boulay S, Colin C, Trentesaux A, et al. Sedimentary responses to the Pleistocene climatic variations recorded in the South China Sea. *Quaternary Research*, 2007, 68: 162-172
 - 17 Hass H C. A method to reduce the influence of ice-rafted debris on a grain size record from Fram Strait, Arctic Ocean. *Polar Res*, 2002, 21: 299-306
 - 18 Clark D, Hanson A. Central Arctic Ocean sediment texture: a key to ice transport mechanisms//Molnia B F. *Glacial-marine Sedimentation*. New York: Plenum Press, 1983:301-330
 - 19 Bischof J F, Darby D A. Mid-to Late Pleistocene ice drift in the Western Arctic Ocean: Evidence for a different circulation in the past. *Science*, 1997, 277: 74-78
 - 20 Nørgaard-Pedersen N, Mikkelsen N, Kristoffersen Y. Arctic Ocean record of last two glacial-interglacial cycles off North Greenland/Ellesmere Island—Implications for glacial history. *Mar Geol*, 2007, 244: 93-108
 - 21 Phillips R L, Grantz A. Regional variations in provenance and abundance of ice-rafted clasts in Arctic Ocean sediments: Implications for the configuration of late Quaternary oceanic and atmospheric circulation in the Arctic. *Mar Geol*, 2001, 172: 91-115
 - 22 Dyke A S, Andrews J T, Clark P U, et al. The Laurentide and Innuitian ice sheets during the Last Glacial Maximum. *Quat Sci Rev*, 2002, 21: 9-31
 - 23 Svendsen J I, Alexanderson H, Astakhov V I, et al. Late Quaternary ice sheet history of northern Eurasia. *Quat Sci Rev*, 2004, 23: 1229-1271
 - 24 Yurco L N, Ortiz J D, Polyak L, et al. Clay mineral cycles identified by diffuse spectral reflectance in Quaternary sediments from the Northwind Ridge: implications for glacial-interglacial sedimentation patterns in the Arctic Ocean. *Polar Research*, 2010, 29: 176-197
 - 25 Knies J, Kleiber H P, Matthiessen J, et al. Marine ice-rafted debris records constrain maximum extent of Saalian and Weichselian ice sheets along the northern Eurasian margin. *Global and Planetary Change*, 2001, 31: 45-64
 - 26 Darby D A, Ortiz J, Polyak L, et al. The role of currents and sea ice in both slowly deposited central Arctic and rapidly deposited Chukchi-Alaskan margin sediments. *Global and Planetary Change*, 2009, 68: 58-72
 - 27 Polyak L, Jakobsson M. Quaternary sedimentation in the Arctic Ocean: Recent advances and further challenges. *Oceanography*, 2011, 24(3):52-64